

Griffith model (eq 11). The inequivalence of these D_{2d} reduced matrix elements is caused by anisotropy in covalency in less than cubic symmetry. When covalent one-electron antibonding orbitals are used to evaluate these reduced matrix elements (eq 13), it is found that the empirically deduced inequality results if the coefficient of covalent mixing for the d_{xy} orbital is greater than that for $d_{xz,yz}$.

Contributions to D in addition to those from ${}^4T_1^{a,c}$ states arise once anisotropic covalency is included in the model. These contributions derive from 6T_1 CT states and the ${}^4T_1^b$ LF state. In the FeCl_4^- complex these contributions individually have non-negligible contributions to D , but the net contribution is small because they oppose each other. The charge-transfer contribution to D is the hardest to obtain because the energies for the states involved must be estimated and because deriving accurate expressions for the SO matrix elements between CT states and the ground state is difficult. Alternatively, the total CT contribution may be estimated experimentally through the use of eq 19 if the g values can be accurately determined. This method should be generally used to estimate the CT contribution to D in systems with low-lying CT states that are strongly low-symmetry-split as is the case for ferric tetrathiolate complexes such as rubredoxin. It is also likely that high-spin ferric heme systems will show a large charge-transfer contribution to D .

Further analysis of the ${}^4T_1^a$ and ${}^4T_2^a$ low-symmetry splittings provides an energy ordering of the one-electron orbitals. It is found that the d_{xy} antibonding orbital is 1300 cm^{-1} above the $d_{xz,yz}$ antibonding orbitals. This is consistent with the compressed D_{2d} geometry of the FeCl_4^- complex, which shifts the ligand $p-\sigma$ bonding orbitals toward the xy plane and away from the xz and yz planes. This is also consistent with the analysis of the sign of D , which leads to the conclusion that the d_{xy} orbital is more covalent than the $d_{xz,yz}$ orbitals. It should be emphasized that the order of the 4T_1 low-symmetry splitting and the anisotropy in covalency are coupled since they both derive from the low-symmetry splitting of the t_2 orbitals (which are σ antibonding in T_d), and thus this effect will always quench the ${}^4T_1^a$ contribution to D in distorted T_d high-spin d^5 complexes.

The final application of the experimental band assignments has been to evaluate the ability of the three-parameter ligand field theory to account for the observed energies. This theory has been remarkably successful when applied to high-spin ions of the first-row transition metals in the +2 oxidation state. But here the spectral fit is not very good, particularly for the higher energy ${}^4T_2^b$ and ${}^4E^b$ states. Such deviations from the predictions of ligand

field theory can also be found in other compounds in the +3 oxidation state (for example, CrX_6^{3-} ; $X = \text{Cl, Br}$).³² These difficulties appear to result from the fact that the electron repulsion parameters appropriate for the free ion do not carry over to molecular symmetry when covalency is significant and that the covalent interactions are stronger in compounds of metal ions in higher oxidation states. Bird and Day³³ have given a more general group theory treatment for electron repulsion in molecular symmetry, but there are too many parameters to evaluate (17 for tetragonal symmetry). That covalency is particularly strong in high-spin d^5 Fe^{3+} is suggested by the very large central field reduction in electron repulsion energies (nephelauxetic effect).³⁴ In particular, the ${}^4E^a$ energy which depends only on electron repulsion terms is only 56% of the energy of the 4G free ion term, whereas in the isoelectronic MnCl_4^{2-} this state occurs at 86% of the 4G energy.³⁵ Unfortunately, there are no theoretical treatments that directly relate coefficients of covalent mixing to the reduction of electron repulsion terms. A second possible source of the significant deviations from the Tanabe–Sugano theory could be spin polarization effects on the antibonding wave functions, which would be larger in a high-spin d^5 ion due to electron exchange interactions. An alternate approach toward describing the bonding in Fe(III) compounds now being pursued is to calibrate $X\alpha$ -SW calculations²⁷ by using the detailed information on the ground and excited states provided by the present spectral study. In particular, the sphere size parameter can be adjusted in these calculations to fit the excited-state transition energies and thus get an experimentally calibrated estimate of the bonding parameters. These calculations should also provide significant insight into the effects of spin polarization on the description of bonding in high-spin d^5 complexes. We anticipate reporting the results of these calculations and their correlation to variable-energy photoelectron spectra in the near future.²⁷

Acknowledgment. We thank the National Science Foundation (Grant No. CHE-8613376) for support of this research. M.S.G. and J.C.D. acknowledge the NSF for graduate research fellowships.

- (32) (a) Wood, D. L.; Ferguson, J.; Knox, K.; Dillon, J. F., Jr. *J. Chem. Phys.* **1963**, *39*, 890. (b) Ferguson, J.; Wood, D. L. *Aust. J. Chem.* **1970**, *23*, 861.
 (33) Bird, B. D.; Cooke, E. A.; Day, P.; Orchard, A. F. *Philos. Trans. R. Soc. London, A* **1974**, *276*, 278.
 (34) Jørgensen, C. K. *Discuss. Faraday Soc.* **1958**, *26*, 110.
 (35) Jørgensen, C. K. *Prog. Inorg. Chem.* **1962**, *4*, 73.

Contribution No. 7809 from the Arthur Amos Noyes Laboratory, California Institute of Technology, Pasadena, California 91125

Excited-State Properties of Dioxorhenium(V). Generation and Reactivity of Dioxorhenium(VI)

H. Holden Thorp, J. Van Houten,[†] and Harry B. Gray*

Received October 17, 1988

The excited-state properties of $\text{trans-ReO}_2(\text{py})_4^+$ (ReO_2^+) in acetonitrile solution have been investigated. The excited-state absorption spectrum of ReO_2^+ is dominated by bleaching of the ground-state MLCT ($(d_{xy})^2 \rightarrow (d_{xy})^1(\pi^*(\text{py}))^1$) and d-d ($(d_{xy})^2 \rightarrow (d_{xy})^1(d_{xz}, d_{yz})^1$) systems. A weak excited-state absorption at $\sim 500\text{ nm}$ is assigned to $(d_{xy})^1(d_{xz}, d_{yz})^1 \rightarrow (d_{xz}, d_{yz})^2$. The reduction potential of $\text{ReO}_2^{2+/+}$ is estimated from emission and electrochemical data to be -0.7 V (SSCE). The ReO_2^+ excited state efficiently ($k_r = 3.6 \times 10^8\text{ M}^{-1}\text{ s}^{-1}$) reduces methylviologen and other pyridinium and olefin acceptors. The recombination electron-transfer reaction is diffusion-controlled ($k_b = 2.1 \times 10^{10}\text{ M}^{-1}\text{ s}^{-1}$). The Re(VI) species ReO_2^{2+} , which can be generated photochemically or electrochemically, is a powerful oxidant. Secondary alcohols and silanes are readily oxidized by ReO_2^{2+} . Acetophenone is the product of *sec*-phenethyl alcohol oxidation.

Introduction

Transition-metal complexes whose excited states undergo electron transfer to form oxidants are under intense study.^{1–5} Our

recent work in this area has centered on $\text{trans-ReO}_2(\text{py})_4^+$ (ReO_2^+ ; $\text{py} = \text{pyridine}$) whose lowest excited state (3E_g) is long-lived (τ

[†] Department of Chemistry, St. Michael's College, Winooski, VT 05404.

(1) (a) Kalyanasundaram, K. *Coord. Chem. Rev.* **1982**, *46*, 159. (b) Meyer, T. J. *Pure Appl. Chem.* **1986**, *58*, 1193. (c) Krause, R. A. *Struct. Bonding* **1987**, *67*, 1.

= 10–15 μ s) in nonaqueous solution.⁶ We have found that the one-electron oxidation of ReO_2^+ , which occurs reversibly at 1.25 V (SSCE) in aqueous solution,⁷ can be effected conveniently by electron transfer from ${}^3E_g \text{ReO}_2^+$ (ReO_2^{+*}) in acetonitrile solution. Further, the d^1 product, ReO_2^{2+} , readily oxidizes secondary alcohols, halocarbons, and silanes.

Experimental Section

Materials. Solvents used for synthesis were reagent grade. Solvents used for physical measurements were freshly distilled from appropriate drying agents under vacuum or an inert atmosphere. KReO_4 (Aesar), tribenzylsilane (Aldrich), and *sec*-phenethyl alcohol (Aldrich, Gold Label) were used as received. Tetra-*n*-butylammonium hexafluorophosphate (TBAH) was prepared by the addition of a dilute HPF_6 solution to a saturated aqueous solution of tetra-*n*-butylammonium bromide. White crystals were obtained after repeated recrystallizations from hot ethanol. Quenchers (mono- and bipyridinium ions, TCNE) were prepared, metathesized, and purified by standard techniques.⁸ Proton NMR spectra were obtained by using a JEOL FX-90Q spectrometer.

$[\text{ReO}_2(\text{py})_4][\text{PF}_6]$. The chloride salt was prepared by the method of Beard et al.⁹ The PF_6^- salt was obtained by addition of a saturated aqueous NH_4PF_6 solution to an aqueous solution of the chloride. The yellow solid was recrystallized from 5:1 acetone/pyridine by the addition of petroleum ether.

Electrochemistry. Cyclic voltammetry measurements were made by using a Princeton Applied Research (PAR) 173 potentiostat and a PAR 175 universal programmer. Platinum-button working electrodes were prepared by polishing with 5- μ m alumina, washing with water, and sonicating in 1:1 MeOH/water. Solutions were degassed with argon and kept under an argon blanket during the experiment. A Pt-wire/glass joint was used to hold the SSCE reference electrode and to prevent water from leaking into the cell. A Pt wire was used as the auxiliary electrode. Solutions were 0.1 M in TBAH and ~ 1 mM in ReO_2^+ . Bulk electrolysis experiments were conducted at a Pt-gauze working electrode by using the PAR 173 potentiostat equipped with a digital coulometer. The bulk electrolysis cell was a two-compartment cell fitted with an argon inlet and a Pt-wire/glass joint for holding the SSCE. Argon flow and stirring were continued throughout the experiment. Electrolysis solutions were exhaustively extracted with pentane for analysis of the organic products by UV spectroscopy. Standard solutions of appropriate concentrations were used for determination of the conversion efficiency.

Photochemical Experiments. Nanosecond laser flash photolysis and resonance Raman experiments were performed at Columbia University in the laboratories of Turro.¹⁰ Time-resolved absorption measurements were made by using 308-nm excitation, and resonance Raman spectra were obtained by using single-pulse 532-nm excitation. Optical absorption spectra were obtained by using a Shimadzu UV-260 recording spectrophotometer. Steady-state photolysis was performed by using a high-pressure Hg/Xe arc lamp equipped with water and air cooling and Corning cutoff filters. Emission spectra were recorded on an instrument that has been described.¹¹ Emission lifetime measurements were made by using a pulsed Nd:YAG system (532-nm excitation).¹² Emission lifetime quenching experiments were performed under vacuum by using a two-compartment cell.¹³

Results and Discussion

Excited-State Properties. The absorption spectrum of ReO_2^+ in acetonitrile solution exhibits a very intense band at 360 nm that is attributable to $d(\text{Re}) \rightarrow \pi^*(\text{py})$ MLCT.^{7,14} A weak band at 416 nm has been assigned to a transition $((d_{xy})^2 \rightarrow (d_{xy})^1(d_{xz},d_{yz})^1)$ to the 1E_g excited state.⁶

Emission from ${}^3E_g \text{ReO}_2^+$ in pyridine, THF, and CH_2Cl_2 so-

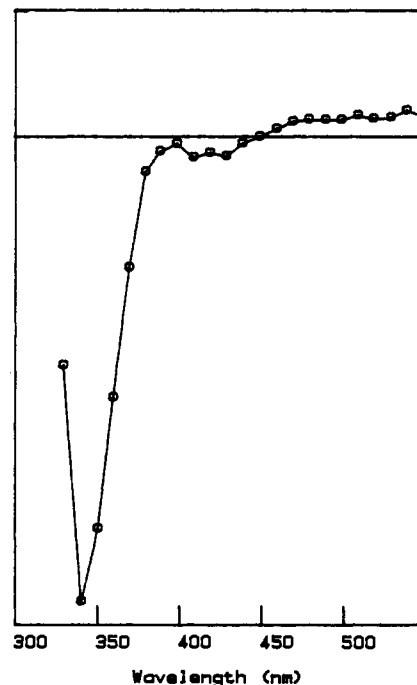


Figure 1. Excited-state absorption spectrum of ReO_2^+ taken 80 ns after 308-nm excitation in CH_3CN .

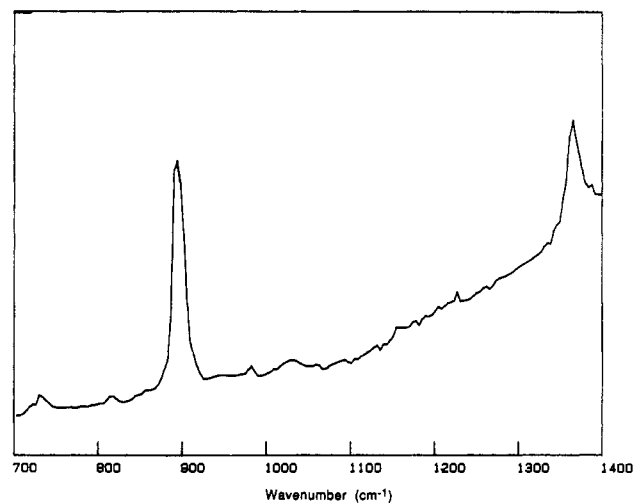


Figure 2. Resonance Raman spectrum of ReO_2^+ in CH_3CN (532-nm excitation).

lutions has been reported.⁶ We have observed similar emission behavior (λ_{max} 640 nm, $\tau = 10 \mu$ s) in acetonitrile solution. Time-resolved absorption spectra taken 80 ns after laser flash photolysis of these solutions are dominated by bleaching of the ground-state MLCT and d-d systems at 340 and 420 nm (Figure 1). This bleaching recovers by first-order kinetics with a lifetime equal to the emission lifetime. A broad, weak excited-state absorption at ~ 500 nm decays with the same lifetime as the emission and the ground-state bleach.

The weak absorption is assigned to a $(d_{xy})^1(d_{xz},d_{yz})^1 \rightarrow (d_{xz},d_{yz})^2$ transition of the 3E_g excited state. On the basis of the energy of the ground-state MLCT, the $\pi^*(\text{py})$ level is estimated to lie $\sim 28400 \text{ cm}^{-1}$ above d_{xy} , thereby placing the energy of the excited-state $(d_{xy})^1(d_{xz},d_{yz})^1 \rightarrow (d_{xz},d_{yz})^2(\pi^*(\text{py}))^1$ transition much higher than that of the observed ~ 500 -nm absorption. Another candidate, $(d_{xy})^1(d_{xz},d_{yz})^1 \rightarrow (d_{xy})^1(\pi^*(\text{py}))^1$, is expected to occur at $\sim 2270 \text{ nm}$ ($\sim 4400 \text{ cm}^{-1}$), which is much lower than the observed band.

The resonance Raman spectrum of ReO_2^+ in acetonitrile solution is shown in Figure 2. This spectrum exhibits a very strong band at 916 cm^{-1} that is assigned to the symmetric Re-O stretch. This frequency is the same as that extracted from the vibronic

- (2) Lees, A. J. *Chem. Rev.* **1987**, *87*, 711.
- (3) Balzani, V.; Bolletta, F.; Scandola, F.; Ballardini, R. *Pure Appl. Chem.* **1979**, *51*, 299.
- (4) Maverick, A. W.; Gray, H. B. *Pure Appl. Chem.* **1980**, *52*, 2339.
- (5) Kavarnos, G. J.; Turro, N. J. *Chem. Rev.* **1986**, *86*, 401.
- (6) Winkler, J. R.; Gray, H. B. *Inorg. Chem.* **1985**, *24*, 346.
- (7) Pipes, D. W.; Meyer, T. J. *Inorg. Chem.* **1986**, *25*, 3256.
- (8) Marshall, J. L. Ph.D. Thesis, California Institute of Technology, Pasadena, CA, 1986.
- (9) Beard, J. H.; Casey, J.; Murmann, K. R. *Inorg. Chem.* **1965**, *4*, 797.
- (10) Kumar, C. V.; Barton, J. K.; Gould, I. R.; Turro, N. J.; Van Houten, J. *Inorg. Chem.* **1988**, *27*, 648.
- (11) Rice, S. F.; Gray, H. B. *J. Am. Chem. Soc.* **1983**, *105*, 4571.
- (12) Nocera, D. G.; Winkler, J. R.; Yocum, K. M.; Bordignon, E.; Gray, H. B. *J. Am. Chem. Soc.* **1984**, *106*, 5145.
- (13) Marshall, J. L.; Hopkins, M. D.; Gray, H. B. *ACS Symp. Ser.* **1987**, *No. 357*, 254.
- (14) Brewer, J. C.; Gray, H. B. Manuscript in preparation.

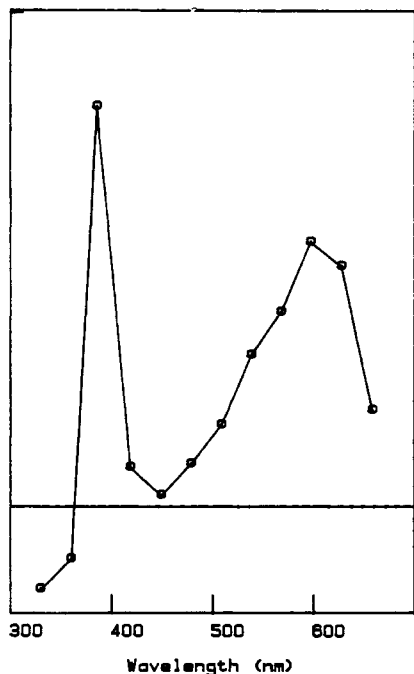


Figure 3. Absorption spectrum of a CH_3CN solution of ReO_2^+ and MV^{2+} taken $2 \mu\text{s}$ after 308-nm excitation.

structure observed in the low-temperature emission spectra of ReO_2^+ in crystals.⁶

Electron-Transfer Reactions. The cyclic voltammogram of ReO_2^+ in 0.1 M TBAH/ CH_3CN solution consists of a single wave at 1.37 V (SSCE) corresponding to a reversible ($\Delta E = 60\text{--}70$ mV, $i_{pc}/i_{pa} \sim 1$) one-electron oxidation. In CH_2Cl_2 solution, however, this wave is only quasi-reversible ($\Delta E \approx 100$ mV, $i_{pc}/i_{pa} < 1$).

With the value of $E_{0-0}(\text{ReO}_2^{2+})$ taken from low-temperature emission data,⁶ the $\text{ReO}_2^{2+}/^{++}$ reduction potential is estimated as³

$$E(\text{ReO}_2^{2+}/^{++}) = E(\text{ReO}_2^{2+}/^+) - E_{0-0}(\text{ReO}_2^{2+}) \approx -0.7 \text{ V (SSCE)}$$

Given this potential, reduction of methylviologen (1,1'-dimethyl-4,4'-bipyridinium, MV^{2+}) should be favored by ~ 0.25 V ($E(\text{MV}^{2+}/^+) = -0.45$ V (SSCE)).⁸ From the Stern-Volmer plot for quenching of the ReO_2^{2+} emission by MV^{2+} , the rate constant $k_t = 3.6 \times 10^8 \text{ M}^{-1} \text{ s}^{-1}$ was obtained.

An electron-transfer reaction is responsible for the quenching of the ReO_2^+ emission. Shown in Figure 3 is the absorption spectrum of an acetonitrile solution of ReO_2^+ and MV^{2+} obtained $2 \mu\text{s}$ after laser flash photolysis. The spectrum contains strong bands at 390 and 600 nm that are attributable to the MV^+ radical.¹⁵ The bleaching at 330 nm is due to ReO_2^{2+} , but it is not as pronounced as that for ReO_2^{2+} .

The rate of MV^+ production determined by the appearance of the transient absorption signals at 390 and 605 nm was first order and agreed with the rate determined by Stern-Volmer emission quenching. The decay trace at 330 nm shows a decrease in bleaching from an initial level due to ReO_2^{2+} to a lower level due to ReO_2^{2+} . This decay is first order and proceeds at the same rate as the increase in absorption due to MV^+ . The disappearance of the MV^+ signal at 605 nm was second order, and least-squares fitting of a $1/[\text{MV}^+]$ plot^{8,16} gives $k_b = 2.1 \times 10^{10} \text{ M}^{-1} \text{ s}^{-1}$ for charge recombination, a rate constant that corresponds to the diffusion-controlled limit in acetonitrile.¹⁷ The extremely efficient recombination is due to the large (~ 1.82 V) driving force for back electron transfer in this system. In addition, k_b also was deter-

Table I. Rate Constants from Stern-Volmer Quenching of the Emission Lifetime of ReO_2^{2+}

Q	$E_{1/2}(\text{Q}^{+/0})$, V vs SSCE ^a	k_t , $\text{M}^{-1} \text{ s}^{-1}$
tetracyanoethylene	+0.24	9.0×10^9
1,10-propylene-1,10-phenanthroline	-0.27	4.5×10^8
1,1'-dimethyl-4,4'-bipyridinium (MV^{2+})	-0.45	3.6×10^8
4-cyano-1-benzylpyridinium	-0.59	2.6×10^8
4-cyano-1-methylpyridinium	-0.67	1.1×10^8
4-carbomethoxy-1-methylpyridinium	-0.78	1.1×10^7
4-amido-1-ethylpyridinium	-0.93	4.1×10^6

^a From ref 5 and 8.

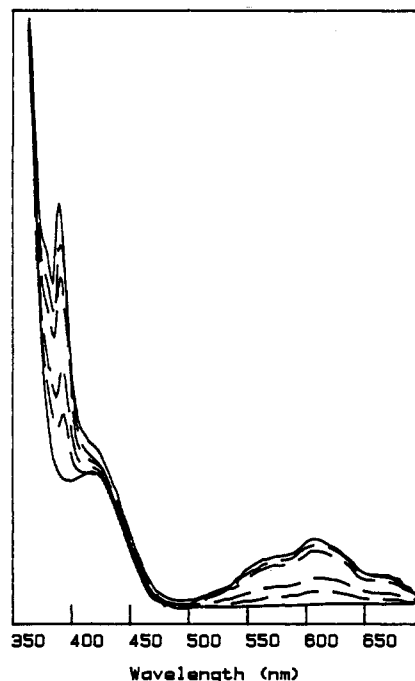


Figure 4. Absorption spectra taken at 15-min intervals during steady-state photolysis of ReO_2^+ and MV^{2+} in CH_2Cl_2 .

mined from the MV^+ signal at 390 nm and the ReO_2^{2+} ground-state bleach at 300 nm. Each of these rate constants is within experimental error of the k_b determined at 605 nm.

The excited state of ReO_2^+ also efficiently reduces other electron acceptors (Table I). The rate constants show that the excited-state reduction potential of -0.7 V (SSCE) estimated from emission and electrochemical measurements is quite reasonable.^{3,17} Further, k_b was estimated for 4-cyano-1-benzylpyridinium, 4-cyano-1-methylpyridinium, and 4-carbomethoxy-1-methylpyridinium. The rate constants indicate that all these reactions (with driving forces > 2.0 V) are diffusion-controlled. Again, the rate constant for the back electron transfer determined from the pyridinium radical absorption was the same as that obtained from the ReO_2^+ ground-state bleach.

Reactivity of ReO_2^{2+} . The oxidation of ReO_2^+ in acetonitrile is reversible on the cyclic voltammetry time scale. This reversibility is supported by the transient absorption experiments. In CH_2Cl_2 , however, the cyclic voltammogram exhibits only a quasi-reversible oxidation wave. Analysis of the scan-rate dependence of this wave¹⁸ indicates that an EC mechanism is operating with a chemical reaction rate of $0.04 \pm 0.01 \text{ s}^{-1}$. Steady-state photolysis of CH_2Cl_2 solutions of ReO_2^+ and MV^{2+} at $\lambda > 450$ nm leads to net production of MV^+ (Figure 4), thereby indicating that ReO_2^{2+} reacts with CH_2Cl_2 in competition with back electron transfer, allowing MV^+ to accumulate. Photolysis of ReO_2^+ and MV^{2+} in THF also led to the production of MV^+ ; however, no absorption

(15) Kosower, E. M.; Cotter, J. L. *J. Am. Chem. Soc.* **1964**, *86*, 5524.

(16) Marshall, J. L.; Stobart, S. R.; Gray, H. B. *J. Am. Chem. Soc.* **1984**, *106*, 3027.

(17) Bock, C. R.; Connor, J. A.; Gutierrez, A. R.; Meyer, T. J.; Whitten, D. G.; Sullivan, B. P.; Nagle, J. K. *J. Am. Chem. Soc.* **1979**, *101*, 4815.

(18) (a) Schwarz, W. M.; Shain, I. *J. Phys. Chem.* **1966**, *70*, 845. (b) Nicholson, R. S. *Anal. Chem.* **1965**, *37*, 1351. (c) Nicholson, R. S.; Shain, I. *Anal. Chem.* **1964**, *36*, 706.

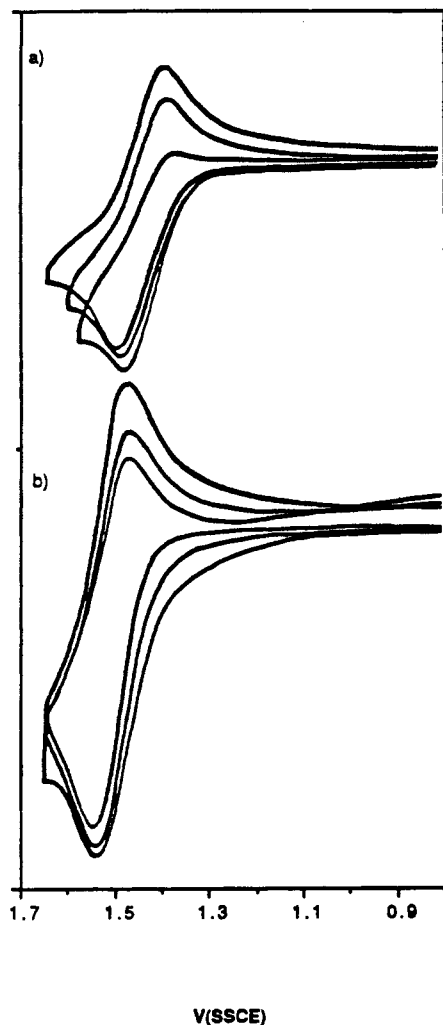


Figure 5. Cyclic voltammograms of ReO_2^+ in CH_3CN with increasing amounts of added (a) $(\text{PhCH}_2)_3\text{SiH}$ and (b) $\text{PhCH}(\text{OH})\text{CH}_3$.

changes were observed after 24 h of irradiation of ReO_2^+ and MV^{2+} in CH_3CN .

The oxidized species, ReO_2^{2+} , also reacts with other organic substrates. Shown in Figure 5a is the oxidation wave of ReO_2^+ with increasing amounts of tribenzylsilane $((\text{PhCH}_2)_3\text{SiH})$ added to the CH_3CN solution. The silane reacts with ReO_2^{2+} , producing an oxidation wave that becomes increasingly irreversible with addition of $(\text{PhCH}_2)_3\text{SiH}$. Figure 5b shows results for a similar experiment performed with *sec*-phenethyl alcohol ($\text{PhCH}(\text{OH})\text{CH}_3$) as the substrate.

Bulk electrolysis of degassed CH_3CN solutions of ReO_2^+ containing $\text{PhCH}(\text{OH})\text{CH}_3$ was performed at $E > 1.5$ V (SSCE). The electrolysis was run for 3 turnovers on the basis of one-electron oxidation of ReO_2^+ . Analysis of the organic products by UV spectroscopy showed that $\text{PhCH}(\text{OH})\text{CH}_3$ was converted to acetophenone. By monitoring of the intense ketone $\pi-\pi^*$ absorption,¹⁹ a current efficiency of $90 \pm 5\%$ for conversion of the alcohol to the ketone (a two-electron process) was determined.

Oxidation Mechanism. A key question is whether a ReO_2^+ -alcohol complex is formed prior to oxidation of the metal complex. Hydrogen bonding of hydroxyl groups to the ReO_2^+ oxo ligands was originally proposed⁶ to explain the quenching of ReO_2^+ emission by molecules containing hydroxyl protons. Figure 6a shows the proton NMR spectrum of *sec*-phenethyl alcohol in CD_3CN . The hydroxyl proton resonance appears as a doublet centered at 3.4 ppm. The α -methylene proton resonance centered at 4.8 ppm is a quartet of doublets due to coupling to the three protons of the terminal methyl group and to the hydroxyl proton.

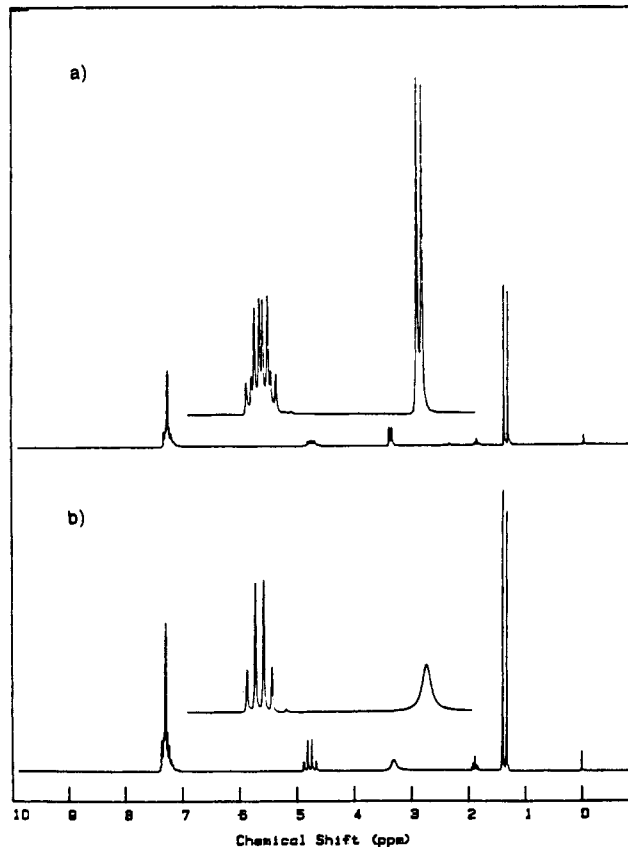


Figure 6. Proton NMR spectra (TMS reference) of (a) *sec*-phenethyl alcohol in CD_3CN and (b) *sec*-phenethyl alcohol in CD_3CN with $\sim 10^{-3}$ equiv of ReO_2^+ added to the solution.

Upon addition of $\sim 10^{-3}$ equiv of ReO_2^+ (Figure 6b), the hydroxyl proton resonance is observed to broaden and to become decoupled from the α -methylene proton resonance, which now appears as a clean quartet due to coupling only to the terminal methyl protons. We have observed that ReO_2^+ also perturbs the hydroxyl proton resonance and coupling in the NMR spectra of related alcohols (phenethyl alcohol, benzyl alcohol, and 1-propanol).²⁰ Similar effects have been reported by Fox et al. in experiments with polyoxotungstate systems.²¹

It is likely that ReO_2^{2+} abstracts a hydrogen atom from the substrate in the initial step of oxidation. One resonance form of ReO_2^{2+} is $\text{Re}(\text{d}^2)$ bonded to an oxo radical, a structure that resembles a carbonyl $\pi\pi^*$ excited state. Recall that $\pi\pi^*$ states efficiently abstract hydrogen atoms from many types of substrates,¹⁹ and $\text{Ru}(\text{IV})$ monooxo and $\text{Ru}(\text{VI})$ and $\text{Os}(\text{VI})$ dioxo complexes undergo the same types of conversions stoichiometrically by H atom abstraction.²²⁻²⁴ The fact that greater than stoichiometric amounts of organic product have been observed under electrolysis conditions indicates that it would be fruitful to search for novel photocatalytic H atom abstraction reactions that could be initiated by electron transfer from ReO_2^{2+} complexes.

Acknowledgment. We thank N. J. Turro and C. V. Kumar for helpful discussions and assistance with the time-resolved absorption and resonance Raman experiments. Stimulating discussions with J. C. Brewer also are acknowledged. H.H.T. is a National Science Foundation Predoctoral Fellow. This research was supported by National Science Foundation Grant CHE84-19828.

(19) Turro, N. J. *Modern Molecular Photochemistry*; Benjamin Cummings: Menlo Park, CA, 1978.

(20) Thorp, H. H.; Van Houten, J. Unpublished observations.
 (21) Fox, M. A.; Cardona, R.; Gaillard, E. *J. Am. Chem. Soc.* **1987**, *109*, 6347.
 (22) (a) Thompson, M. S.; DeGiovani, W. F.; Moyer, B. A.; Meyer, T. J. *J. Org. Chem.* **1984**, *49*, 4972. (b) Dobson, J. C.; Seok, W. K.; Meyer, T. J. *Inorg. Chem.* **1986**, *25*, 1514.
 (23) (a) Che, C.-M.; Yam, V. W.-W.; Cho, K. C.; Gray, H. B. *J. Chem. Soc., Chem. Commun.* **1987**, 948. (b) Yam, V. W.-W.; Che, C.-M.; Tang, W.-T. *J. Chem. Soc., Chem. Commun.* **1988**, 100.
 (24) Marmion, M. E.; Takeuchi, K. J. *J. Am. Chem. Soc.* **1988**, *110*, 1472.